Int. J. Electron. Commun. (AEÜ) 132 (2021) 153609

Contents lists available at ScienceDirect

International Journal of Electronics and Communications

journal homepage: www.elsevier.com/locate/aeue

Regular paper

Nonreciprocal filtering power dividers☆

Jiawei Zang [a], Shouyuan Wang [a], Alejandro Alvarez-Melcon [b,*], J. Sesbastian Gomez Diaz [c]

[a] China Academy of Information and Communications Technology, Beijing 100191, China
[b] Communications and Information Technologies Department, Universidad Politécnica de Cartagena, Campus de la Muralla del Mar s/n, Cuartel de Antigones, Cartagena 30202, Región de Murcia, Spain
[c] Department of Electrical and Computer Engineering, University of California at Davis, Davis, CA 95616, USA

ARTICLE INFO

Keywords:
Filtering power dividers
Spatio-temporal modulation
Time-modulated resonators
Nonreciprocal devices
Magnetless nonreciprocity

ABSTRACT

We propose the concept of nonreciprocal filtering power dividers, which are compact devices able to merge the functionalities of power dividers and combiners, the selectivity of bandpass filters, and magnetless non-reciprocity from time-modulation. A prototype of this type of devices operating at microwaves has been implemented in microstrip technology. The device is composed of a Wilkinson power divider integrated with two identical microstrip filters based on quarter-wavelength coupled lines. The resonators of the filters are terminated with varactors that are time-modulated using low-frequency harmonic signals from a Coplanar Waveguide (CPW) feeding network printed on the ground plane of the microstrip structure. The resulting compact device behaves as a nonreciprocal power divider, nonreciprocal power combiner, or a common filtering power divider depending on the modulation parameters. In addition, it exhibits electrical frequency reconfigurability (over 15%), high rejection out of the passband, and enhanced isolation among the ports. A manufactured prototype shows relative fractional bandwidth of 3.1% measured at a return loss level of 11 dB, and insertion losses of 5.9 dB, together with a nonreciprocal response with over 21 dB of directivity at the center frequency.

1. Introduction

Filters and power dividers are essential devices in many communication systems. To improve the integration and reduce fabrication costs of such systems, multifunctional filtering power dividers possessing both frequency selectivity and power division have attracted significant interest [1–5]. On the other hand, nonreciprocal components, such as circulators, have been traditionally based on the use of magnetic and ferrite materials [6]. More recently, however, magnetless and complementary metal-oxide-semiconductor (CMOS) processing compatible circulators [7,8] based on time-modulation have recently been proposed and experimentally demonstrated aiming to enable full-duplex communication systems. Additional magnetless nonreciprocal components, such as microwave filters [9,10] and antennas [11], have just been developed and experimentally verified.

In this context, we propose the concept of nonreciprocal filtering power dividers: a compact and integrated device able to combine the functionalities of power-dividers and bandpass filters with magnetless nonreciprocity. This device provides significant advantages to implement integrated and CMOS-compatible communication systems, including a very compact size, relatively low-loss, frequency reconfigurability, improved isolation among ports compared to common power dividers, and the ability to behave as a nonreciprocal power combiner or divider at will. Filtering power dividers and magnetless nonreciprocity based on time-modulation are independent research topics that have attracted significant attention by the scientific community [12]. However, most of these works are related to the development of circulators [13]. Within the frame of this research, this paper proposes a compact structure behaving as a nonreciprocal filtering power divider, which integrates the functionalities of power dividers, the selectivity of bandpass filters, and isolators simultaneously. This is the first time such a device is reported to the authors knowledge.

It should be noted that the proposed device exhibits higher insertions losses than other previously reported filtering power dividers, such as [1–3]. However, our design integrates the additional functionality of an isolator, and the non-reciprocity characteristics improve the natural isolation between ports. Also, the device proposed in [2] is suitable for wideband operation, while the proposed circuit in this work operates

☆ CPW: Coplanar Waveguide, CMOS: Complementary Metal-Oxide-Semidonductor, RF: RadioFrequency, FPGA: Field Programmable Gate Array.

* Corresponding author.
E-mail addresses: zangjiawei@caict.ac.cn (J. Zang), wangshouyuan@caict.ac.cn (S. Wang), alejandro.alvarez@upct.es (A. Alvarez-Melcon), jsgomez@ucdavis.edu (J.S. Gomez Diaz).

https://doi.org/10.1016/j.aeue.2021.153609
Received 9 July 2020; Accepted 8 January 2021
Available online 2 February 2021

naturally in narrow band, similar to [3]. In the following, we provide useful guidelines for the design of this type of components together with the fabrication and characterization of a prototype operating at microwaves.

2. Design and Implementation

Fig. 1(a) depicts the schematic of the proposed nonreciprocal filtering power divider, which is composed of a Wilkinson power divider terminated on the output ports (2 and 3 in the figure) with identical nonreciprocal bandpass filters based on time-modulation [9,10]. The Wilkinson divider works at the RF signal f_{RF}, and can be designed with standard techniques [14]. The design includes a resistor of value of $2Z_0$ placed between the two quarter wavelength impedance transformers (with characteristic impedance $\sqrt{2}Z_0$ at the operation frequency) to introduce impedance matching for ports 2 and 3 and keep them isolated. Nonreciprocity is triggered, by modulating with low frequency (f_m) signals, the resonators that compose the bandpass filters, as illustrated in Fig. 1(b).

A specific implementation in microstrip technology of the proposed device is shown in Fig. 2. A conventional microstrip Wilkinson power divider and two identical third order quarter wavelength microstrip coupled lines filters are printed on the top layer of an F4B substrate with relative dielectric constant $\varepsilon_r = 2.55$, dielectric loss tangent $\tan\delta = 0.0015$, and thickness of 1.27 mm. The reference impedance of the three RF ports operating at f_{RF} is $Z_0 = 50\ \Omega$. The resonators that compose the filters can be time-modulated: the quarter wavelength coupled lines are terminated with varactors that are fed with low-frequency signals coming from a coplanar network printed on the ground plane. Photographs of the fabricated prototype are shown in Fig. 2(b).

The embedded biasing structure used to feed the modulation signals, is based on coplanar waveguide transmission lines (CPW) opened in the ground plane of the microsrip structure. The characteristic impedance of each CPW is set to 50 Ω with $w = 3$ mm and $g_4 = 0.2$ mm [see Fig. 2(a)] to match the 50 Ω SMA connector. For each modulation path, an inductor, which functions as a lowpass filter, is employed. In this way, the modulation signals as well as the DC bias voltages can be efficiently fed to all varactors, while the RF signals are prevented from leaking into the modulation sources. Note that an additional DC block component is not necessary in this bias circuit because the DC voltage source is inherently isolated due to the capacitive coupled lines filter structure.

Applying reversed DC bias voltages and time varying modulation signals to the varactors, the capacitance of the i-th varactor can be expressed as

$$C_i(t) = C_0\,[1 + \Delta_m \cos(2\pi f_m\, t + \varphi_i)\,] \tag{1}$$

where C_0 is the static capacitance determined by the DC bias voltage (V_{DC}), and $\Delta_m = \Delta C/C_0$ is the modulation index ($0 < \Delta_m < 1$) with ΔC being the maximum capacitance variation controlled by the amplitude of the modulation signal. Modulation signals with identical frequency (f_m) and amplitude are applied to all resonators. In addition, an incremental modulation phase ($\Delta\varphi$) is applied between consecutive resonators, leading to different phases of the form $\varphi_i = (i-1)\,\Delta\varphi$, with i = 1, 2, 3, [see Fig. 1(b)].

The Skyworks SMV1232 varactors located on the bottom layer are connected to the coupled line resonators through metallic vias (0.4 mm in diameter). As shown in Fig. 2, six coplanar waveguides are built on the bottom ground plane to carry the modulation signals as well as the DC bias common to all varactors. For each modulation path, an inductor (52 nH) is employed as an RF choke to improve f_{RF}-f_m isolation (31 dB measured value).

Strong nonreciprocal transmission can be achieved by properly tuning the frequency (f_m), modulation index (Δ_m), and phase increment ($\Delta\varphi$) of the modulation signals. Nonreciprocity is induced into the system due to nonreciprocal couplings and phase cancellation effects among the generated nonlinear harmonics in the time-modulated resonators of the filters, as described in [10].

For the design of the complete device, the Wilkinson divider and the two bandpass filters are first designed separately. Both components are designed for a center frequency of $f_{RF} = 2.4$ GHz, and in the case of the filters with Tchebyshev responses of 11 dB of return losses, and fractional bandwidths of 6.5%. After this initial design phase, both components are integrated together, and a final optimization is carried out to compensate for parasitic couplings and higher order interactions. The final dimensions of this prototype are given in the caption of Fig. 2.

3. Results and performance

Without applying modulation signals, the proposed filtering power divider is reciprocal. Fig. 3a shows the static response of the device. Good filtering performance is observed together with high selectivity. In these plots, measured results are compared with linear numerical simulations obtained with HFSS, observing good agreement. In particular, the measured passband (S_{21}) is centered at 2.4 GHz with a relative bandwidth of 7.3% measured at a return loss level of 11 dB. The in-band minimum insertion loss of the filter (without including the division loss) is 2.4 dB. The isolation between ports 2 and 3 (S_{32}) is higher than 28 dB within the entire passband. The measured results in the right panel show that the magnitude imbalance between the two output ports (2 and 3) is less than 0.3 dB and the maximum phase difference is less than 6.8° within the passband. In addition, note that symmetry considerations lead to $S_{21} = S_{31}, S_{22} = S_{33}$, whereas reciprocity imposes that $S_{32} = S_{23}$,

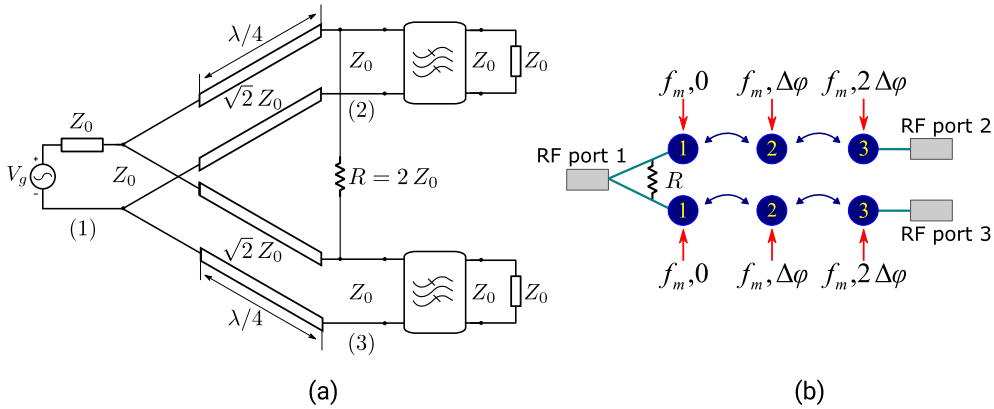

Fig. 1. Block diagrams of the proposed nonreciprocal filtering power divider. (a) Wilkinson power divider connected to two identical filters on ports (2) and (3). (b) Nonreciprocity is achieved by introducing a time modulated signal into the resonators of both filters. Modulation signals have the same modulation index Δ_m and frequency f_m, but a progressive phase shift $\Delta\varphi$ is applied between resonators of same filters.

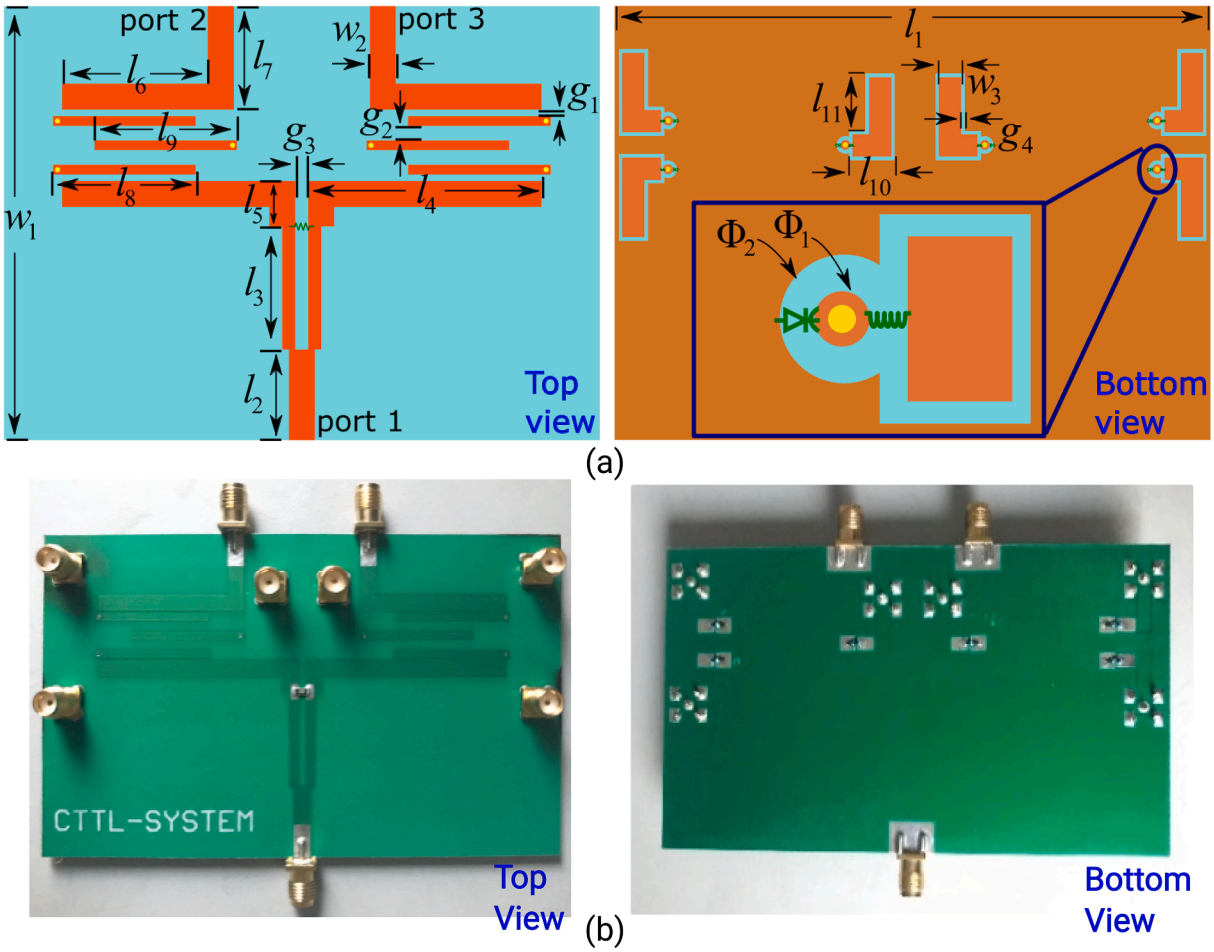

Fig. 2. Proposed nonreciprocal filtering power divider in microstrip technology. Dimensions in mm: $l_1 = 114, l_2 = 15, l_3 = 20.4, l_4 = 43.7, l_5 = 6.7$, $l_6 = 28.3, l_7 = 16.7, l_8 = 25, l_9 = 24.4$, $l_{10} = 8, l_{11} = 10.3, w_1 = 69.4, w_2 = 3.4, w = 3$, $g_1 = 0.5, g_2 = 2.4, g_3 = 1.6, g_4 = 0.2$, $\Phi_1 = 1, \Phi_2 = 2$. (a) Geometry of the proposed divider. (b) Photograph of the fabricated divider.

$S_{21} = S_{12}$ and $S_{31} = S_{13}$.

To achieve nonreciprocal operation between port 1 and output ports 2–3 (i.e., $S_{21} \neq S_{13}$ and $S_{31} \neq S_{13}$), time-modulation is applied to the three resonators that compose each bandpass filter. The modulation parameters are optimized using the procedures described in [9,10] leading to $V_{DC} = 1.8$ V (to give $C_0 = 2.09$ pF), $f_m = 90$ MHz, $\Delta_m = 0.09$, and $\Delta\varphi = 80°$. The measured responses of the proposed nonreciprocal filtering power divider are shown in Fig. 3(b). Simulation results obtained by combining linear simulations from HFSS [15] and nonlinear circuit analysis from ADS Keysight [16] are also shown for validation, obtaining good agreement with respect to measurements.

Very good out-of-band rejection is observed in the modulated state. An 11 dB return loss level bandwidth of 3.1% centered at 2.4 GHz is achieved. The minimum extra insertion loss in S_{21} is 5.9 dB (3.5 dB more than in the static situation). The extra insertion loss is due to losses in the varactors and biasing elements (choke inductors) as well as some residual power that is converted into higher order harmonics and is not converted back into the fundamental frequency [9,10]. Strong nonreciprocity is obtained between S_{21} and S_{12} with a directivity larger than 21 dB at the center frequency and larger than 10 dB in the entire bandwidth of 2.3%. It should be noted that the nonreciprocal response of the filters helps to improve the isolation between output ports 2 and 3 (S_{32}), which is enhanced over 18 dB and achieves a value larger than 46 dB in the whole bandwidth. It is seen that the measured magnitude imbalance of the two output ports is below 0.4 dB, while the phase difference is less than 6°.

Note that the relatively high losses obtained in this device are due to the low quality factors exhibited typically by microstrip printed resonators [17], and by the narrow bandwidth achieved (3.1% fractional bandwidth). In general, the parameters of the modulation signals (f_m, Δ_m and Δ_φ) can be optimized to enlarge the bandwidth, and thus improve the return losses. However, as described in [10], there is a trade-off between the achievable bandwidth and the directivity that can be obtained in a given design. We emphasize that spatio-temporal modulation is a relatively narrow band technique. For instance, recent acoustic nonreciprocal filter proposed in [18] exhibits a fractional bandwidth of only 1.7%.

The direction of transmission in the proposed nonreciprocal filtering power divider can be reversed by simply changing the sign of the phase increment applied to the resonators of the filters (i.e., $\Delta\varphi = -80°$). The measured results in this situation are shown in Fig. 4. We can see that very similar responses are obtained in terms of insertion losses, return losses, isolation between ports, directivity and ports imbalance. Again, measured results are presented together with simulations for validation. This test shows that the device can be easily reconfigured to function as a nonreciprocal power combiner, by just changing the sign of the phase increment applied to the resonators.

An additional feature of the proposed nonreciprocal filtering power divider is frequency reconfigurability. Such reconfigurability can easily be realized in two steps. First, the desired operational frequency range can be adjusted by changing the DC voltage (V_{DC}). Second, fine tuning of the modulation parameters (f_m, Δ_m, and $\Delta\varphi$) is performed to recover an optimal nonreciprocity response. Fig. 5 shows two specific cases of frequency reconfigurability. The modulation parameters obtained in

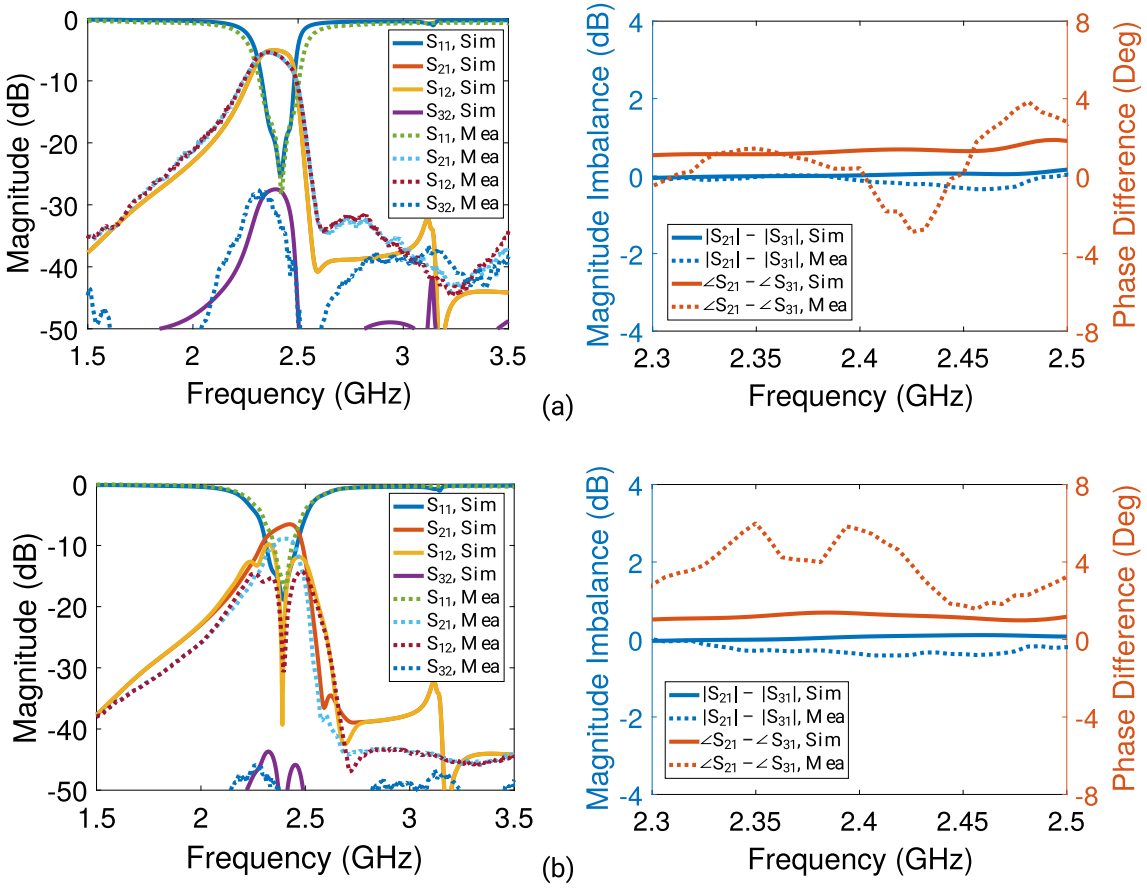

Fig. 3. Response of the proposed nonreciprocal filtering power divider. (a) Static response. (b) Modulated response.

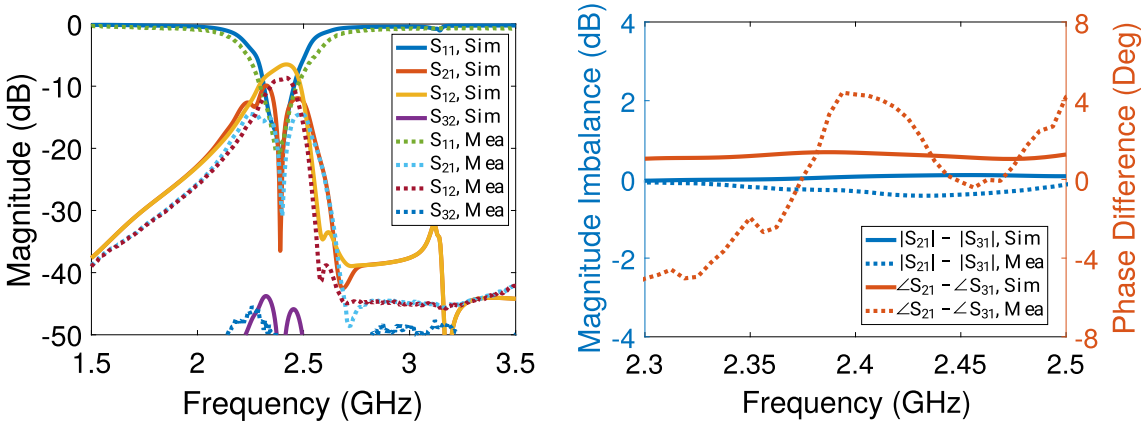

Fig. 4. Response of the proposed nonreciprocal filtering power divider with reversed modulation phases. In this mode the device works as a nonreciprocal power combiner, since it can combine the signals present at ports (2) and (3) into port (1), while rejecting any signal present at port (1).

measurements are $V_{DC} = 0.4$ V (3.3 V), $f_m = 88$ MHz (95 MHz), $\Delta_m = 0.08$ (0.11), and $\Delta\varphi = 88°$ (82°) for Fig. 5(a) (Fig. 5(b)).

As observed, when V_{DC} increases, the center frequency where the device operates also increases, due to the lower C_0 value provided by the varactors. In this situation, both the modulation index (Δ_m) and the modulation frequency (f_m) need to be slightly increased to recover the isolation. This is due to the higher coupling coefficients that occurs in this type of filters when the center frequency increases, which result in wider absolute bandwidths of the static responses. In any case it is observed that, by adjusting appropriately the modulation parameters, the device performance in terms of insertion loss, return loss, isolation, and magnitude and phase imbalance between ports, is still good over the entire tuning range (15%). Note that these optimized parameters could be easily programmed, for instance in an FPGA or other configurable processors, to obtain a real time reconfigurable device.

Important parameters that should be evaluated when integrating non-linear devices, are both the power handling and the non-linearity properties with input power levels. In general, the power handling of the proposed nonreciprocal filtering power divider is mainly limited by the nonlinearity of the varactors [19]. To check this nonlinearity behavior, we present the simulated input-referred 1-dB compression point (P1dB), the input-referred third-order intercept point (IIP3), and

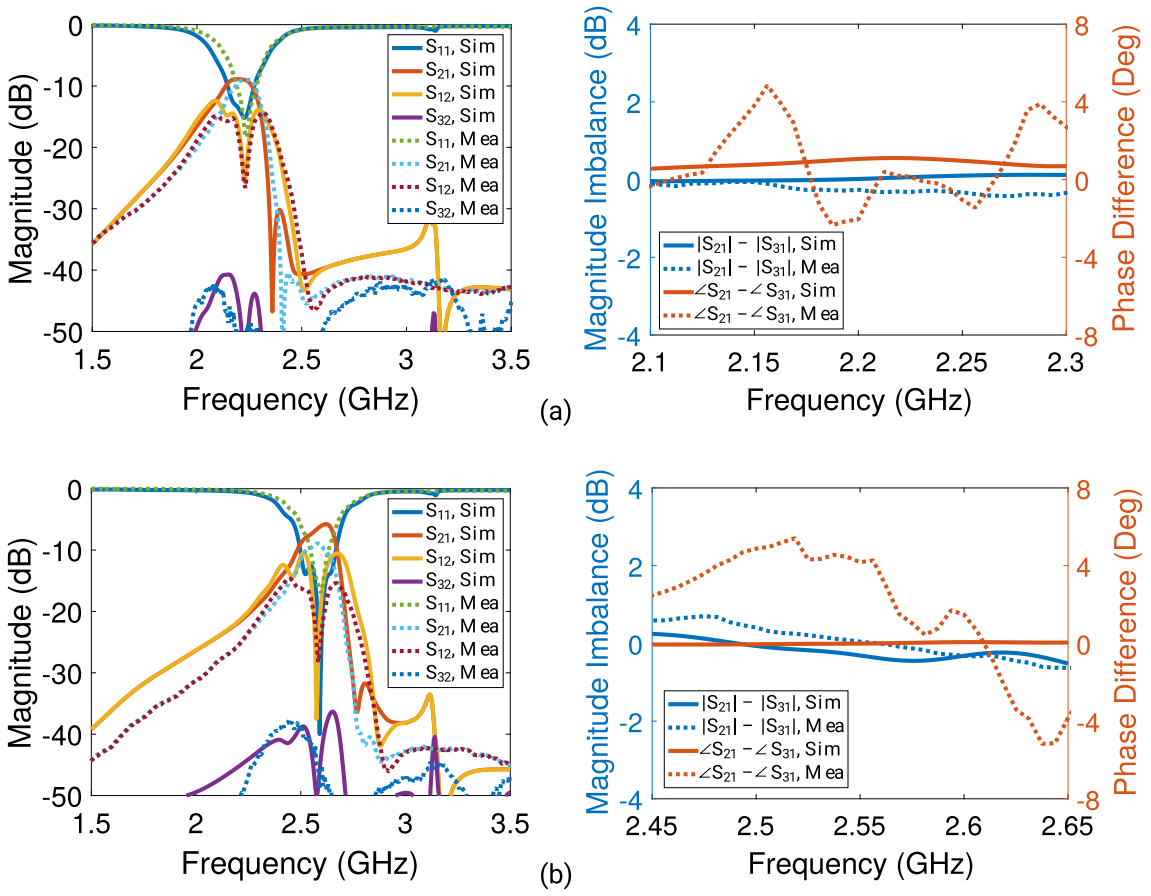

Fig. 5. Frequency reconfigurability capabilities of the proposed circuit. (a) Decreased DC bias voltage ($V_{DC} = 0.4$ V). (b) Increased DC bias voltage ($V_{DC} = 3.3$ V).

the noise figure (NF), in Fig. 6. These plots are obtained using the harmonic balance (HB) simulation in ADS. The IIP3 simulations is done with two signals at 2375 MHz and 2425 MHz. The simulated P1dB is approximately 17 dBm and the IIP3 is approximately 18.5 dBm. A moderate value of NF = 5.3 dB is obtained at the center frequency of 2.4 GHz. Compared with other structures previously reported in the literature, the proposed device in this paper exhibits high linearity (i.e. P1dB of 10.9 dBm was reported in [20], and P1dB of 9.2 dBm and IIP3 of 11.8 dBm is demonstrated in [21]). With respect to NF, our device shows a better performance than the results reported in [22] with an NF value of 21.2 dB.

In any case, these results show that our proposed device behaves within the state of the art, of recently reported components achieving non-reciprocity by using non-magnetic techniques.

4. Conclusions

A compact nonreciprocal filtering power divider based on time modulated resonators has been proposed and experimentally demonstrated. The device integrates a Wilkinson power divider with two identical filtering structures implemented with coupled lines quarter-wavelength microstrip resonators. High compactness is achieved by feeding the low frequency modulation signals through CPW lines integrated in the ground plane of the microstrip lines. Measured results from a manufactured prototype confirms the performance of this type of devices, which combine the functionalities of nonreciprocal power divider and combiner, and exhibit high selectivity out of the passband, enhanced isolation among the ports, and electrical reconfigurability. The measured prototype has demonstrated fractional bandwidth of 3.1% measured at a return loss level of 11 dB, and a bandwidth of 2.3% with

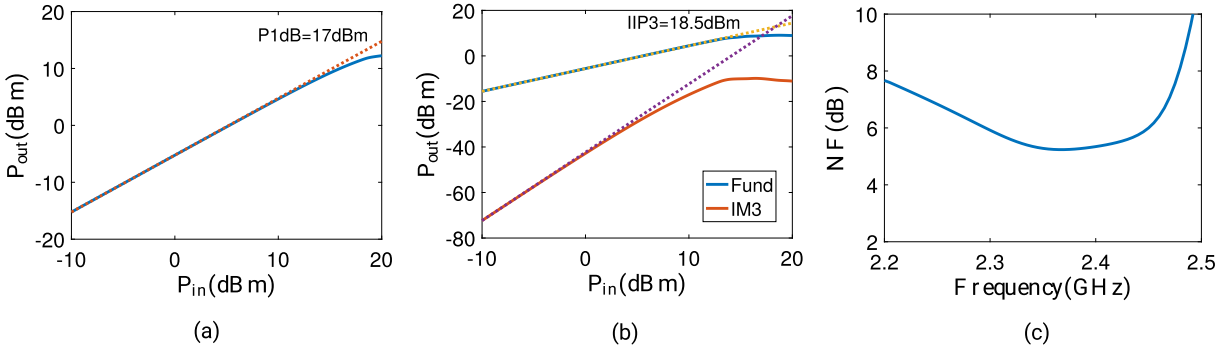

Fig. 6. Non-linear behavior of the proposed non-reciprocal filtering power divider. (a) Input-referred 1-dB compression point. (b) Input-referred third-order intercept point. (c) Noise figure.

directivity larger than 10 dB. Moreover, it is shown that the induced nonreciprocity increases the isolation between the output ports 2 and 3 over 18 dB. In addition, the device exhibits electrical reconfigurability with a tuning range of 15%. We envision that the proposed device may find exciting applications in emerging communication systems that require the integration of several functionalities in compact structures.

Contributors

J. Zang started the basic research with the integration of a Wilkinson power divider with two nonreciprocal filters. He also did the manufacturing tasks and the experiments, and contributed to the writing of the manuscript. S. Wang participated in the design and in the experimental tasks of the device. He also contributed to corrections in the manuscript. A.A. Melcon contributed to the theory of nonreciprocal filters, and to the writing of the manuscript. J.S.G. Diaz contributed to the theory of spatio-temporal modulations and also performed corrections and improvements in the manuscript. All authors have approved the final article.

Declaration of Competing Interest

The authors declare that they have no known competing financial interests or personal relationships that could have appeared to influence the work reported in this paper.

Acknowledgment

The authors gratefully acknowledge financial support from Ministerio de Economia y Competitividad of Spain and the European Regional Development Funds for their financial support (Grant No.: PID2019-103982RB-C42). The work was partially supported by the National Science Foundation with CAREER Grant No. ECCS-1749177. This work was supported by the National Natural Science Foundation of China under Grant 62001520.

References

[1] Li Y, Xue Q, Zhang X. Single and dual-band power dividers integrated with bandpass filters. IEEE Trans Microw Theory Techn 2012;61:69–76. https://doi.org/10.1109/TMTT.2012.2226600.
[2] Song K, Mo Y, Zhuge C, Fan Y. Ultra-wideband (UWB) power divider with filtering response using shorted-end coupled lines and open/short-circuit slotlines. AEU Int J Electron Commun 2013;67(6):539. https://doi.org/10.1016/j.aeue.2012.12.002.
[3] Shen G, Feng W, Che W. Compact filtering power divider with extended stopband using out-of-phase feeding scheme. Electron Lett 2019;55(25):1347–9. https://doi.org/10.1049/el.2019.3077.
[4] Lu D, Yu M, Barker N, Mei L, Shi-Wen T. A simple and general method for filtering power divider with frequency-fixed and frequency-tunable fully canonical filtering-response demonstrations. IEEE Trans Microw Theory Techn 2019;67(5):1812–25. https://doi.org/10.1109/TMTT.2019.2903504.
[5] Vaziri H, Zarghamib S, Shama F, Kazemi A. Compact bandpass Wilkinson power divider with harmonics suppression. AEU Int J Electron Commun 2020;117 (153107):1–10. https://doi.org/10.1016/j.aeue.2020.153107.
[6] Marynowski W, Kusiek A, Mazur J. Microstrip four-port circulator using a ferrite coupled line section. AEU Int J Electron Commun 2009;63(9):801–8. https://doi.org/10.1016/j.aeue.2008.06.008.
[7] Estep NA, Sounas DL, Soric J, Alu A. Magnetic-free non-reciprocity and isolation based on parametrically modulated coupled resonator loops. Nat Phys 2014;10 (12):923–7. https://doi.org/10.1038/NPHYS3134.
[8] Kord A, Tymchenko M, Sounas D, Krishnaswamy H, Alu A. CMOS integrated magnetless circulators based on spatiotemperal modulation angular-momentum biasing. IEEE Trans Microw Theory Techn 2019;67(7):2649–62. https://doi.org/10.1109/TMTT.2019.2915074.
[9] Wu X, Liu X, Hickle MD, Peroulis D, Gomez-Diaz JS, Melcon AA. Isolating bandpass filters using time-modulated resonators. IEEE Trans Microw Theory Techn 2019;67 (6):2331–45. https://doi.org/10.1109/TMTT.2019.2908868.
[10] Melcon AA, Wu X, Zang J, Liu X, Gomez-Diaz J. Coupling matrix representation of nonreciprocal filters based on time modulated resonators. IEEE Trans Microw Theory Techn 2019;67(12):4751–63. https://doi.org/10.1109/TMTT.2019.2945756.
[11] Zang J, Alvarez-Melcon A, Gomez-Diaz J. Nonreciprocal phased-array antennas. Phys Rev Appl 2019;12(054008):1–20. https://doi.org/10.1103/PhysRevApplied.12.054008.
[12] Kord A, Sounas D, Alu A. Microwave nonreciprocity. IEEE Proc 2020;108(10): 1728–58. https://doi.org/10.1109/JPROC.2020.3006041.
[13] Kord A, Sounas DL, Alu A. Magnet-less circulators based on spatiotemporal modulation of bandstop filters in a delta topology. IEEE Trans Microw Theory Techn 2018;66(2):911–26.
[14] Pozar DM. Microwave Engineering. John Wiley and Sons; 1998. ISBN: 0-471-17096-8.
[15] Ansoft, HFSS 12.0; 2020. http://www.ansys.com/Products/Electronics/ANSYS-HFSS.
[16] Technologies Keysight. ADS - Advanced Design System. Santa Rosa, CA, USA: EEsof; 2019. https://www.keysight.com.
[17] Hong J, Lancaster M. Microstrip filters for RF/Microwave Applications. USA: John Wiley & Sons; 2001.
[18] Cassella C, Michetti G, Pirro M, Yu Y, Kord A, Sounas DL, Alu A, Rinaldi M. Radio frequency angular momentum biased quasi-LTI nonreciprocal acoustic filters. IEEE Trans Ultrason Ferroelectr Freq Control 2019;66(11):1814–25.
[19] Wu L-S, Zhou X-L, Yin W-Y, Tang M, Zhou L. Characterization of average power handling capability of bandpass filters using planar half-wavelength microstrip resonators. IEEE Microw Wireless Compon Lett 2009;19(11):686–8.
[20] Wu X, Nafe M, Melcon AA, Gomez-Diaz JS, Liu X. Frequency tunable non-reciprocal bandpass filter using time-modulated microstrip $\lambda_g/2$ resonators. IEEE Trans Circ Syst II: Express Briefs 2020:1–6. https://doi.org/10.1109/TCSII.2020.3014499.
[21] Yang C, Gui P. 85–110 GHz CMOS magnetic-free nonreciprocal components for full-duplex transceivers. IEEE J Solid-State Circ 2019;54(2):368–79.
[22] Wang Y, Chen W, Chen X. Highly linear and magnetless isolator based on weakly coupled nonreciprocal metamaterials. IEEE Trans Microw Theory Techn 2019;67 (11):4322–31.